Journal of Shipping and Ocean Engineering 6 (2016) 323-338
doi 10.17265/2159-5879/2016.06.002

Recent Advances to Change the Standards in Designing Hulls in Waves, a Validation Using an Efficient SWENSE Level-Set Approach

Ivan Schrooyen[1], Mikael Berton[2] and Karl Randle[1]

1. ULSTEIN DESIGN & SOLUTIONS, Ulsteinvik/Norway

2. LEMMA, Biot/France

Abstract: This paper presents recent naval applications of the SWENSE (Spectral Wave Explicit Navier-Stokes Equations) approach implemented for the first time with high order fully unstructured schemes and an efficient level-set method to capture free surface flows around realistic hull geometries. Numerical simulations in waves and/or viscous flows still lead generally to very large CPU times because of grid requirements to ensure a good propagation of incident waves in the meshed part of the fluid domain that makes unreachable any hull design optimization process in an industrial context. Furthermore, even if the SWENSE method clearly shows promising results in an academic context in both regular and irregular waves, the most recent publications still highlight several issues that remain unresolved up to now, e.g. poor scalability, diffusive wake pattern, non-versatile structured mesh approaches and only very few validation test cases are carried out on Wigley or DTMB 5415 hulls. In order to overcome those numerical difficulties and get an in-depth validation of the method on several cases in realistic wave conditions, a two and a half years' research project has been achieved involving several steps, starting by a set of dedicated model test experiments later used as reference for the validation of the method. The CFD commercial code ANANAS™ used and developed in this research program is presented and validated in detail. The use of high order schemes on unstructured grids in combination with these SWENSE method and level-set approach offer to the maritime industry an innovative and state of the art method to achieve unequaled accuracy, low computation time and some unique advantages such as, amongst others, the end of the numerical wave propagation problems. The results of the validation were pleasing and can be considered as acceptable in general, with some challenges remaining to the solved. Results obtained indicate that an optimization processes in waves in realistic conditions is now affordable in an industrial context.

Key words: CFD simulation, SWENSE, level-set, ship design, optimization, waves, added drag.

1. Motivation

Over the last century, Ulstein has developed some expertise and reputation within the ship design industry. The business was for a long time mainly oriented towards offshore solutions. Depending on the type of design (e.g. PSV (platform supply vessel), Wind Support Vessel, Construction Vessel, etc.) the optimum hydrodynamic solution might be very different. Indeed, Wind Support and Construction Vessels do operate most of the time in DP (dynamic positioning) mode so that the designer needs a good understanding of the flow at zero speed in waves. On the other hand, for PSV, the understanding of hydrodynamic phenomena in transit is equally important as DP. This transit is commonly split into calm water transit and transit in waves.

The conventional method applies strip theory, potential theory based on linear wave response theory and empirical methods in the different loops of the ship design process while model tests were only conducted during the final design loop. Satisfactory hydrodynamic learning can of course be achieved by attending and questioning model test experiments, however these are quite seldom and expensive.

Furthermore, conventional theory neglects the volume and buoyancy distribution above the

Corresponding author: Ivan Schrooyen.

waterplane, which is of interest for the time varying forces and motions. The methods proposed here consider the entire vessel above and below water.

The broadening of the business areas to Exploration Vessels, Yachts and Cruise Vessels requires some different hydrodynamic expertise. The use of appropriate numerical methods (CFD) can boost the learning phase and bring Ulstein straight into the competition with well optimized solutions.

Accurate CFD methods to quickly estimate the calm water performance of a vessel are known and available on the market for a while. A confirmed user can expect to get his resistance predictions within the same uncertainty margin as experiments (typically 3%) and therefore perform quick, cheap and reliable calm water optimizations.

However, most designs rarely operate in calm water conditions and optimizing a vessel in waves is a totally different matter. In order to succeed in the task, the designer needs a tool that will deliver the right information (typically forces and motions). Other requirements for the tool are the following: an affordable price for a relatively small ship design company, consistent results (a small change in the numerical parameters should lead to negligible changes to the physical results), the possibility to access detailed flow visualizations, some automation possibilities (via scripts), a low computation time, robustness, competent support, and a proper validation of the tool leading to clearly established guidelines. In addition, the aim is to industrialize a scientific tool for an engineer with a limited knowledge of CFD to make complex calculations. The tool would ideally reach a comparable uncertainty level as experiments (typically 5% on the average forces in waves). Even though this might seem unnecessary, comparing similar designs in an optimization process with a tool that suffers from 15-20% uncertainty levels can be seen as a pretty hazardous task.

This paper aims at presenting the CFD method that Ulstein Design & Solutions has chosen to exploit to perform these simulations, and its extensive validation, in collaboration with an established provider of CFD software.

2. Overview of the SWENSE Approach

The SWENSE (Spectral Wave Explicit Navier-Stokes Equations) approach has been developed since 2003 by the HOE (Hydrodynamics & Ocean Engineering) group of ECN (Ecole Centrale de Nantes). In the SWENSE method, incident wave terms are computed with a potential flow model and are then introduced explicitly in an RANSE solver whose equations have been modified by decomposing each physical variable in the sum of an incident variable and a diffracted one. The diffracted field is the only unknown solved by the modified RANSE code. Details of this method can be found in Ref. [1] and has been validated on numerous test cases (e.g. Luquet [2] and Monroy [3]) using the CFD software ICARE [4] based on a finite difference second order structured scheme. Reliquet et al. [5] introduce the level-set method to describe the free surface using the same CFD code, showing the potential of this method on a classical benchmark (DTMB 5415) on two cases (one in steady resistance at Fr = 0.28 and one in head waves). Even if the potential of the SWENSE strategy is clearly shown in the last paper and thesis, more validations (non-linear regular and irregular waves, different hull headings) are needed to assess its global accuracy. Last but not least, several issues highlighted in the previous papers still remain and are considered as major drawbacks when regarding practical industrial needs and intensive calculations:

- Structured mesh approaches definitely lead to several issues when complex geometries must be handled and often limit the success of a high automation level;
- The very first speed-up tests achieved by Monroy [3] exhibit very poor results (efficiency falls around 50% on 16 cores) and could be explained either by the code structure or a consequence of the total field

decomposition imposed in the SWENSE method;

- The free surface resolution obtained with the proposed level-set approach shows a very diffusive pattern around the hull and in the wake even if the drag and pressure force are well predicted.

To overcome these three main shortcomings, Lemma implemented the SWENSE approach in ANANAS™ software, a mixed finite element finite volume CFD code based on unstructured high order schemes whose features are described in section 3. The above leading to easy meshing of complex geometries, good scalability (see section 5) and detailed free surface visualizations.

3. Physical Modeling within the ANANAS™ Solver

Computations are run using ANANAS™ which solves the incompressible balance equations for mass and momentum. The flow modelling relies on a Level Set formulation [6, 7], of a two-fluid incompressible flow as introduced in Ref. [8]. ANANAS™ uses tetrahedral elements and is based on a mixed finite volume finite element method. Time integration is carried out using a third order explicit scheme while space integration is handled with the V6 high order scheme introduced by Koobus et al. [9] which yields to sixth order for uniform mesh spacing. The turbulence is modelled with a high Reynolds k-epsilon SST model as proposed by Francescatto et al. [10]. For accuracy purpose, the Reichardt analytical law [11] was chosen since it gives a smooth matching between linear, buffer and logarithmic regions. Because the y+ normalized distance is generally subject to large variations in complex geometries, it has been considered as mandatory to combine together wall law and low Reynolds modelling which locally damps the fully-turbulent model in regions in which the wall law does not cover the buffer zone.

This code has proven its efficiency to solve numerous problems in hydrodynamics such as free-surface flows [8, 12, 13] and turbulence around offshore platforms [14].

In the SWENSE approach presented here, incident wave terms are computed with a potential flow model [15] for a non-linear regular waves and with the JONSWAP directional spectrum for irregular waves). These are then introduced explicitly in the ANANAS™ solver whose equations have been modified to fulfil the decomposition of each physical variable in the sum of an incident variable and a diffracted one. The diffracted field is the only unknown solved by the code. This approach combined with the highly parallelized unstructured numerical schemes used in ANANAS™ leads to the following advantages:

- The numerical wave propagation problems usually handled through a so-called direct method (wave maker) do not exist anymore;
- The domain size can be very small since the only diffracted waves need to be damped;
- The engineer can refine his mesh on the vessel only, no other cells are needed (except for detailed visualization);
- SWENSE coupled to the level-set approach allows breaking wave and complex free surface representation in a versatile multi-domain framework;
- The implicit high order scheme used to discretise the momentum and advection equations leads to an accurate representation of the free surface, as a contrary to the diffusive wake pattern previously obtained by Monroy [3] or Reliquet et al. [5];
- Finally, the CPU time required to handle a simulation in waves compared to more classical approaches can be divided by 2 to 15 depending on the simulated wave length as well as geometry complexity. This speed-up and code efficiency have been studied and observed for different mesh sizes up to 5 million points so far. Besides that, high order schemes allow the user to get converged results with a smaller number of nodes compared with low order schemes that are classically used in naval hydrodynamics with dominated hex mesh and schemes limited to order 2 in space and time.

4. Description of the Validation Method

This validation work is based on a set of dedicated model scale experiments performed at HSVA in Germany in such a way that they can be reproduced in CFD without any assumption that would have significant impact on the results. Ulstein has ordered this set of tests and attended them carefully to achieve sufficient understanding of the experiments to perform a successful numerical validation, and avoid lengthy discussions later. CFD calculations are performed in model scale to allow direct comparisons, even though full scale characteristics of the ship and wave conditions are reported in order to give a more physical understanding to the reader.

The 3D model used for this validation work is the Ulstein PX121 which is a common product of Ulstein's portfolio. To reduce validation costs, a single model has been used in the tank. However, considering 0 degree and 180 degree headings gives two very different hydrodynamic shapes that can be considered as two separate "designs". The 3D model (Fig. 1) was equipped with two tunnel thrusters with sharp edges as well as two headboxes. The pod units were not present during the tests. The vessel characteristics are presented in Table 1.

The experimental set-up of HSVA consists in a horizontal towing frame (Fig. 2) built for CFD validation purposes and that has the advantages to be flexible with the control of the degrees of freedom and the measurement of forces and motions. A 3 DOF set-up is used for this validation. The pitch and heave are free while surge motion is restrained by a linear spring. The spring characteristics (stiffness, damping and inertia) were all taken into account in the CFD calculations. The use of a spring in the system was necessary to ensure high quality force measurements and has the two additional advantages to be more physical and to make the CFD validation more general. It is important to note that the spring stiffness was tuned to ensure its resonance frequency was not excited by the wave frequency.

Surge, pitch and heave (including their respective derivatives) have been measured throughout the tests as well as the longitudinal force evolution. It is interesting to note that the force measurements in this set-up are fully redundant. Indeed, the measurements of the surge motion coupled with the known characteristics of the spring allow to rebuild the force signal and perform cross checks. This aspect has been exploited through the validation process.

Numerical reproducibility of the experiments was essential to ensure direct comparison of the EFD and CFD. Consequently, a significant portion of the physical testing was made in regular waves. Additional tests were made in irregular waves to make the validation as general as possible. Waves of 2.5 m are the most probable in the North Atlantic [16] which oriented Ulstein's choice to select this wave height for the validation. On top of that, waves of 4 m height still represent common working conditions in the winter so that this wave height has been added to the validation. Simulations are therefore based on these two wave heights. Considering the industrial needs, two wave periods have been selected for each wave height, the first one being a classical long wave and the second one

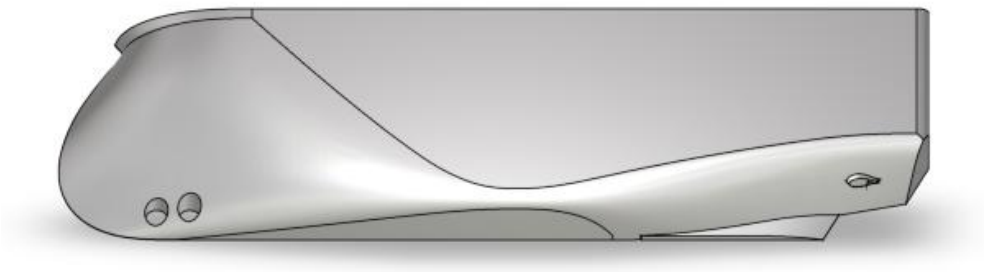

Fig. 1 View of the 3D model.

Table 1 Main particulars of the Ulstein PX121 (full scale).

Characteristic	Value
Length between perpendiculars LOA	83.3 m
Breadth in waterline B	18.0 m
Draught T	6.0 m
Displacement ∇	5,759.2 m^3

corresponding to the steepest non-breaking wave that the basin could simulate. The capability to simulate harsh conditions is indeed key in the design process, while being a typical difficulty for numerical simulations. The wave characteristics are presented in Table 2.

Wave calibrations have been performed prior to the tests using a probe moved through the tank at the position where the vessel would be in order to ensure a sufficient number of successive wave encounters respecting the target wave height with a maximum deviation of 5%. For steep waves that naturally tend to become unstable and therefore less regular, it was necessary to accept fewer wave encounters (typically 15) and select the right time window in which steady conditions were achieved.

Headings of 0 degree and 180 degrees have been considered in this validation with the convention that a 180 degrees heading corresponds to a wave impacting the bow. Half of the simulations have been performed

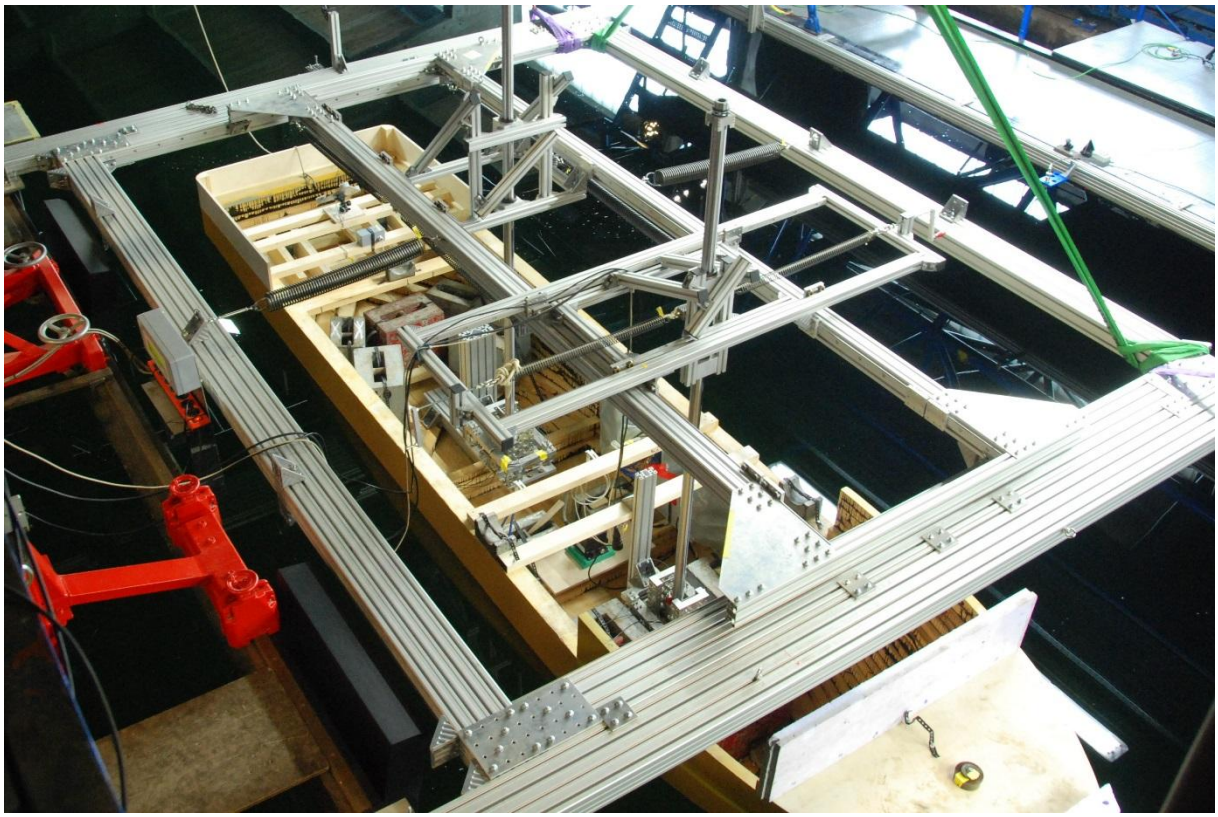

Fig. 2 Top view of the arrangement in the HSVA large towing tank.

Table 2 Wave characteristics (full scale).

Wave height $H_{(s)}$ [m]	Wave period $T_{(p)}$ [s]	Wave length λ [m]	Wave steepness $H_{(s)}/\lambda$ [-]	Wave type
2.5	5.5	47.2	0.053	Regular “steep”
2.5	9.5	140.9	0.018	Regular “long”
2.5	9.5	140.9	0.018	JONSWAP ($\gamma = 3.3$)
4.0	6.5	66.0	0.061	Regular “steep”
4.0	10.0	156.1	0.026	Regular “long”

at 0 average speed to simulate DP operation, while the other half were performed with the vessel moving towards the waves at 8 kt and 10 kt (which corresponds to Fr = 0.15 and Fr = 0.18). The experiments with the stern moving towards the waves were conducted at reduced speed (5 kt / Fr = 0.09) to stay realistic. A couple of calm water resistance tests (forwards and backwards) have been added to the scope to be able to deduce the wave added resistance.

It is important to be aware that the use of a spring in the experimental set-up introduces a transient that will be different for the EFD than for the CFD due to the different initial condition. Consequently, only converged and RMS values can be compared.

Accuracy of both experiments and numerical simulations has always been an entertaining point of contention between model test basins and CFD vendors, the contention being of course more intense when observing a poor match between EFD and CFD. It will remain a moot point for many years, in the same way as comparing EFD results from different model test basins or comparing numerical predictions from different codes. Trying to keep a neutral position on that matter, and based on error calculations, basins comparisons, experiment repetitions with different measurement set-ups and in-house experience, Ulstein estimates the maximum relative uncertainty around the forces measurements to be around 5%. For the cases showing a wide range of force variation with a low average value (typically in long waves at zero speed), one must consider the maximum absolute uncertainty which is estimated around 1.5 Newton. Similarly, a maximum uncertainty of 0.25 degree around the dynamic pitch angle as well as 5 millimeters around the dynamic heave measurements will be considered for this set of experiments.

In order to set an accessible objective, the choice has been made to allow a similar uncertainty around the CFD predictions and as a consequence to aim at getting all CFD predictions within 10% from EFD when focusing on the average forces in waves. Without going into deep uncertainty quantification theory, such an achievement on a large number of comparisons does not prove that the CFD has achieved an accuracy of 5%, but conclusions would go towards that direction.

Searching for an average drag of a couple of Newtons based on a time signal oscillating between values that are sometimes two orders of magnitude above requires a rigorous post-processing. Two distinct methods have been used to perform the post-processing and have been applied in the same way to both EFD and CFD. The first method is a short-term Fourier transform while the second is being defined by Eq. (1) and both methods return the same converged result for the mean value.

$$\boldsymbol{F_x(\tau)} = \frac{\sum_{i=0}^{N} \int_{\tau - T + \frac{iT}{N}}^{\tau + \frac{iT}{N}} \boldsymbol{F_x(t)dt}}{\boldsymbol{N+1}} \qquad (1)$$

Eq. (1) is the definition of the sliding average over time which has the advantages to eliminate the target frequency, to be systematic and to give the same importance to each point of the input curve. However, the main disadvantage is that the average over time cannot be defined during the first and last periods T of the original signal.

5. Validation of the CFD Results

The twenty-three validation cases are presented in Table 3 which is split in three parts, describing DP simulations, calm water resistance and transit in waves. The cases have been chosen to be representative of the physical possibilities and include some difficult cases on purpose. In particular, the case #20 was expected to be hydrodynamically complex while important to the validation and has therefore been repeated twice in the tank, which gives an indication on the experiments repeatability (about 1.5% on the average force in this case). The case #21 corresponds to a PX121 backing at 5 kt into steep waves of 4 m height, which is an extreme case, but was tested to push the limits of both experiments and CFD. For such a seldom condition in the vessel operational profile, the fuel consumption

Table 3 List of validation experiments (full scale).

Case #	Vessel speed [kt] / Fr [-]		Wave height $H_{(s)}$ [m]	Wave period $T_{(p)}$ [s]	Heading [deg]	Wave type
01	0		2.5	5.5	180	Regular "steep"
02	0		2.5	5.5	0	Regular "steep"
03	0		2.5	9.5	180	Regular "long"
04	0		2.5	9.5	180	JONSWAP (γ = 3.3)
05	0		4.0	6.5	180	Regular "long"
06	0		4.0	6.5	0	Regular "steep"
07	0		4.0	10.0	180	Regular "long"
08	0		4.0	10.0	0	Regular "long"
09	8	0.15	-	-	-	Resistance
10	10	0.18	-	-	-	Resistance
11	12	0.22	-	-	-	Resistance
12	14	0.25	-	-	-	Resistance
13	16	0.29	-	-	-	Resistance
14	-5	0.09	-	-	-	Resistance
15	-10	0.18	-	-	-	Resistance
16	8	0.15	2.5	9.5	180	Regular "long"
17	10	0.18	2.5	9.5	180	Regular "long"
18	-5	0.09	2.5	9.5	0	Regular "long"
19	10	0.18	2.5	9.5	180	JONSWAP (γ = 3.3)
20	10	0.18	4.0	6.5	180	Regular "steep"
21	-5	0.09	4.0	6.5	0	Regular "steep"
22	10	0.18	4.0	10.0	180	Regular "long"
23	-5	0.09	4.0	10.0	0	Regular "long"

aspect (average force) is irrelevant, while the main concern is the water on deck which is a danger for the crew and equipment.

The realization of the numerical domain and CFD meshes has been a non-intuitive task in the sense that the previous experience acquired by using VOF codes had to be partly left on the side in order to take full advantages of the SWENSE—level set formulation. Indeed, the concept is based on the superposition of the incoming waves (prescribed analytically) and the diffracted waves (solved by modified RANS). Consequently, the diffracted fields are the only ones requiring numerical damping. Moreover, these diffracted fields have a lower magnitude, allowing shorter numerical damping zones, all around the vessel. Finally, prescribing the incident fields totally eradicates the well-known numerical wave propagation problems (large numerical domains, difficulties to maintain the wave height, grid size, time step, especially for steep waves and zero speed cases). The combination of these two advantages leads to a unique domain size (non-dimensionalized by the vessel length), used for all types of simulations: DP in waves, calm water resistance and transit in waves. The resulting numerical domain is shown in Fig. 3. All tests being symmetric configurations, only half of the geometry has been modeled.

The CFD meshes have been generated with ANAMESH™ being part of the ANANAS™ package developed by Lemma. This mesh generator has the capability to easily generate anisotropic unstructured tetrahedral meshes based on the metric concept. The technique offers the flexibility to fully control the mesh in any location. In particular, the user has the possibility to impose different discretization levels on the physical entities of their geometry and control the way the mesh is coarsened in any vicinity (gradation). The gradation is important to capture the different

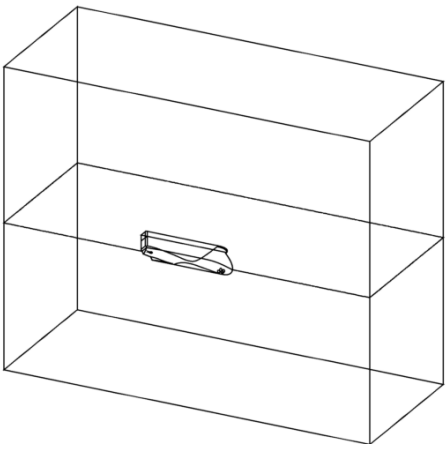

Fig. 3 Illustration of the numerical domain.

gradients in the ships' vicinity. In addition, any mathematical and/or logical function can be defined to impose the evolution of the spatial discretization, leading to smooth transitions between refined and coarse regions.

Systematic mesh convergence studies have been carried out to understand the mesh requirements on the different physical entities of the vessel, the needed gradation as well as the mesh in the volume and specifically for the free surface.

An indication of the mesh density on the hull is presented in Fig. 4. This plot is obtained by making a logarithmic representation of the cell volume inverse. Another non-intuitive finding is that the mesh density has a pretty low impact on the final result as long as the geometry is well captured which means that mesh convergence is achieved pretty early. This finding is most probably a direct consequence of the use of a high order solver. The flat transom creates a voluminous detachment while transiting in waves that justifies some additional local refinements.

A similar plot is presented on Fig. 5 for the free surface. The most important finding related to the SWENSE method was that the vertical discretization on the free surface (cell height) is not as critical as for other tools. Therefore, the vertical discretization is chosen to have enough cells to capture diffracted waves (in the ship vicinity) and enough cells to capture the main wave height further away. As a direct consequence, reflected waves are progressively damped further from the vessel, helping the additional numerical damping system. The same applies to the horizontal discretization that needs to be sufficient to capture diffracted wave lengths in the ship vicinity and the main wave length further away. The anisotropy is reduced behind the transom.

Finally, Fig. 6 gives an idea of the mesh density under the ship where a slight refinement has been performed to take into account the added mass.

These mesh requirements are actually so light that the choice has been made to refine horizontally more

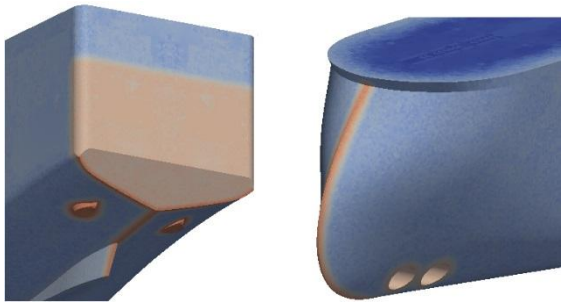

Fig. 4 Indication of the mesh density on the hull.

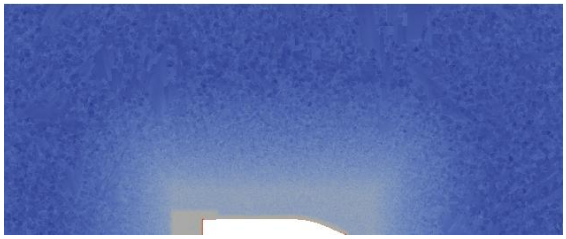

Fig. 5 Indication of the mesh density on the horizontal cur at the free surface level.

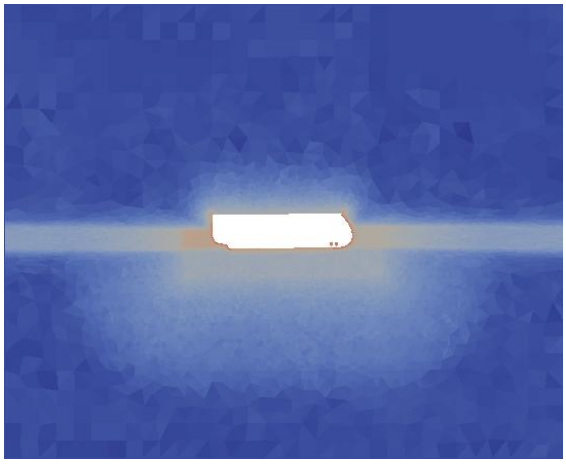

Fig. 6 Indication of the mesh density on the symmetry plane.

than required on the free surface and use the same mesh for different wave periods (wave lengths). The free surface refinement thickness remains obviously dependent on the wave height, leading to three different meshes for calm water resistance, transit in 2.5 m waves and transit in 4.0 m waves. A point has been reached where visualization is driving the cell count more than result accuracy.

The vessel motions induced by wave excitation in DP involve velocities that are low enough to justify the Euler hypothesis (by direct tests on a selection of zero speed cases with and without viscous effects, there was less than 1% variation on the force results). The outcome of this comparison is the possibility to generate meshes without viscous layers and consider the ship surfaces as slip walls for these cases, maintaining confidence in the results. In addition to the aforementioned viscous meshes, two additional Euler meshes are generated for 2.5 m and 4 m waves in DP. The characteristics of the meshes used for this validation are presented in Table 4.

Classical mesh deformation techniques are applied to the system to allow the vessel motions in pitch, heave and surge. Their implementation is made in such a way that mesh deformations do not affect the CPU time in a significant way.

Given the steepness of some waves of the scope, it was important to use a numerical formulation that can deal with highly non-linear waves. Rienecker & Fenton waves have shown to be particularly suitable to model all regular wave cases and gave a good agreement with experimental waves. Irregular waves have been modeled using a JONSWAP spectrum (γ = 3.3), as in the experiments.

Taking advantage of the SWENSE formulation, it is not necessary to wait for the waves to propagate through the CFD domain and in order to avoid numerical shocks, the incident fields (wave height, velocity and pressure) are progressively grown in a "non-physical way" during 1 wave period. Simulations in regular waves are then run for 20 wave periods which is sufficient to achieve proper convergence (steady average as defined in Eq. (1)).

Calculations have run on a Linux cluster system, using 64 cores each and leading to the computation times presented in Table 5. The overall cluster capacity includes 256 cores dedicated to parallel computations and a couple of other servers used for pre- and post-processing. The servers used for parallel computations include 16 cores each (2x Intel Xeon E5-2680 @ 2.7 GHz) and 128 Gb of RAM (16x8 Gb RDIMM 1600 MHz). Efficient communication between servers is ensured by InfiniBand. A well configured queuing system helps dispatching the jobs

Table 4 Characteristics of the CFD meshes.

Mesh #	Case # (cf. Table 3)	Mesh size [Mpts]	Usage
01	01, 02, 03, 04	2.21	DP in 2.5 m waves
02	05, 06, 07, 08	2.16	DP in 4.0 m waves
03	09, 10, 11, 12, 13, 14, 15	3.55	Resistance ahead and backwards
04	16, 17, 18, 19	4.50	Transit in 2.5 m waves
05	20, 21, 22, 23	4.32	Transit in 4.0 m waves

Table 5 Computational time.

Case #	Wave encounters [-]	Computation time [Hrs]
01, 02, 03, 05, 06, 07, 08	20	15-20
04	100	89
09, 10, 11, 12, 13, 14, 15	-	Function of Fr number
16, 17, 18, 20, 21, 22, 23	20	70
19	100	250

and keeps the cluster occupation close to 100% all over the year.

Moreover, the scalability of ANANAS™ has been tested on the case #02 (mesh #01), leading to the results presented on Fig. 7 and Table 6. The calculation set-up has been reviewed to remove unnecessary disk access (such as volume probes) and limit the simulation time to two wave periods. The cluster was running these simulations only, and each point of the curve has been repeated three times on different nodes (when possible). On top of the super-convergence phenomenon when using 2 cores, it is important to note that the highest efficiency is obtained with 64 cores (around 35,000 mesh points per core) and that this efficiency is 95%. Other relevant points for industrial work (32 cores, 128 cores and 256 cores) show an efficiency remaining above 74% which is satisfactory. Finally, the use of heavier meshes (#03, #04 and #05) shows higher efficiency when using 128 and 256 cores.

During the validation process, post-processing has become an unexpected challenge. Indeed, the objective is to run unsteady simulations and keep some 3D information 50 times per period in order to be able to dig into the flow by making different types of smooth animations. Such a frequency represents about 1,000 sets of 3D information for a regular-wave simulation and about 4,000 sets for an irregular-wave simulation. To keep the highest possible efficiency of the nodes processing the parallel calculation, it was necessary to save the full 3D solution without additional time consuming manipulations. Saved results are therefore partitioned as the mesh. To offer unlimited post-processing possibilities, the choice has been made to save volumic solutions. However, such an approach is not sustainable since 4 parallel calculations are most of the time running at the same time, creating a couple of Gb of data every 5 minutes. Ulstein has therefore developed some post-processing scripts that detect when a volumic solution is written on the storage system, load and reassemble the 3D solution in one block, extract some key surfaces from it (typically free surface, cutting planes and vessel) along with key information (typically velocity, pressure, wave elevation, turbulent viscosity), save the 2D results in a light file and finally remove the heavy 3D file from the storage system. Such jobs are launched in parallel in a queue including 32 cores which are sufficient to handle the data produced by the 256 parallel cores. Finally, other post-processing scripts use the same queue of 32 cores to turn these 2D files into animations based on user requests in 5 to 10 minutes. Examples of such unsteady post-processing are available on Ulstein website:
https://ulstein.com/ship-design/customised-designs/cfd-simulations.

Scripting of the CFD tasks is definitely key in the

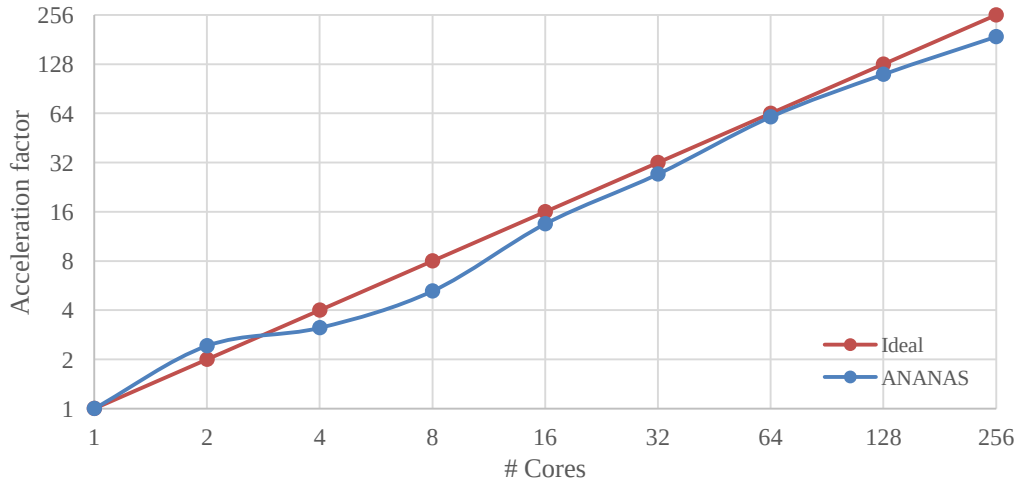

Fig. 7 Acceleration curve of ANANAS™ based on case #02.

Table 6 Scalability of ANANAS™ based on case #02.

# Cores	Efficiency [%]	Acceleration [-]
1	100	1
2	121	2.4
4	78	3.1
8	65	5.2
16	84	13.5
32	85	27.2
64	95	60.9
128	87	111.0
256	74	188.6

design process in order to ensure consistency, save time and limit the number of human errors. In addition to the scripting of post-processing tasks, the whole chain has been automated, including meshing and computation set-up. Smart non-dimensionalisation work has been required to achieve wise scripting. Typical input parameters to the scripts are fluid properties, the hull model itself and its main dimensions, the ship draught and speeds, as well as the wave characteristics (height, period, type). It is important to note that the software has not been tuned to achieve good results, and as a consequence, these parametric guidelines apply to the various wave heights, wave periods, ship speeds and headings tested.

Overall results are presented in Table 7 where Fx corresponds to the average force in the longitudinal direction estimated with Eq. (1), Ry is the pitch motion range of the model and Tz is the heave range motion. For irregular wave cases (#04 and #19), the reported values of Ry and Tz are RMS values and do not correspond to the motion ranges.

Focusing on the DP simulations to start with (cases #01 to #08), one might notice a good agreement meeting initial expectations on the average forces and motions. Moreover, relative differences with experiments do not show any trend of systematic under- or over-prediction of the results which represents another advantage of the method. Finally, a

Table 7 Comparison of the EFD and CFD results.

		EFD			CFD		
Case #	Fx [N]	Ry [deg]	Tz [m]	Fx [N]	Ry [deg]	Tz [m]	Rel Diff Fx
01	27.0	1.46	0.041	25.3	1.18	0.047	-1.7 N
02	41.0	2.80	0.028	40.3	2.52	0.032	-1.7%
03	1.6	5.02	0.127	1.5	5.13	0.130	-0.1 N
04	3.0	1.14	0.029	3.9	1.13	0.032	0.9 N
05	59.9	5.04	0.069	65.5	5.24	0.113	9.4%
06	74.4	5.29	0.04	70.1	4.89	0.077	-5.8%
07	3.4	7.54	0.218	3.2	7.38	0.215	-0.2 N
08	2.6	7.59	0.228	4.2	7.42	0.211	1.6 N
09	37.9	0.06	-0.006	37.3	0.07	-0.006	-1.6%
10	59.4	0.10	-0.009	59.3	0.11	-0.010	-0.2%
11	93.6	0.20	-0.013	92.6	0.20	-0.014	-1.0%
12	143.6	0.25	-0.018	143.6	0.30	-0.020	0.9%
13	230.9	0.31	-0.025	230.9	0.38	-0.028	2.3%
14	22.7	0.00	-0.002	23.1	0.00	-0.003	1.5%
15	108.5	0.01	-0.031	108	0.06	-0.011	-0.5%
16	82.6	6.08	0.151	76.0	6.65	0.114	-8.7%
17	113.8	6.41	0.172	116.4	7.25	0.148	2.3%
18	32.5	5.76	0.132	31.2	6.13	0.108	-4.0%
19	99.5	1.52	0.04	99.7	1.55	0.038	0.2%
20	235.3	3.34	0.032	214.9	2.80	0.045	-8.7%
21	269.5	4.39	0.076	337.5	4.73	0.081	25.2%
22	132.0	9.52	0.287	150.0	9.80	0.260	13.6%
23	42.0	8.19	0.237	43.1	9.5	0.252	2.6%

detailed look at the cases #07 and #08 highlights that the CFD is more able to capture small relative differences than experiments. Indeed, it is expected to have a higher average force when the waves impact the flat transom (case #08) than when the waves impact the bow (case #07), which is well predicted by the CFD but not by the EFD.

An example of surge force signal is given on Fig. 8 for the case #2 where the average force signal has been superposed according to Eq. (1). The signal demonstrates that proper convergence of the force average has been achieved.

Fig. 9 presents the diffracted wave elevation for the case #02 at a given time. The result has been scaled back to full scale for easier understanding. Such a representation is quite unusual and shows the capabilities of the SWENSE method to highlight some physical phenomena such as the waves generated by the vertical movement of the stern. These waves travel in the opposite direction compared to the incoming waves. The second important phenomenon is observed in the ship wake where the diffracted waves are in phase opposition with the incoming waves, forming a physical sheltered zone. One might notice a green zone

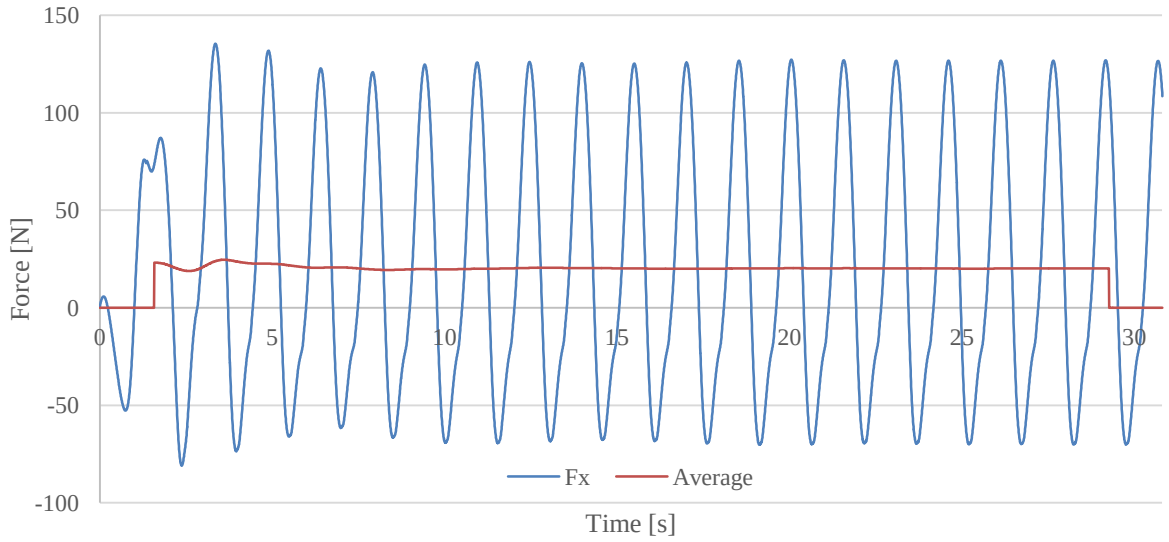

Fig. 8 Evolution of the surge force (Fx) and average force (Average) along time for the case #02.

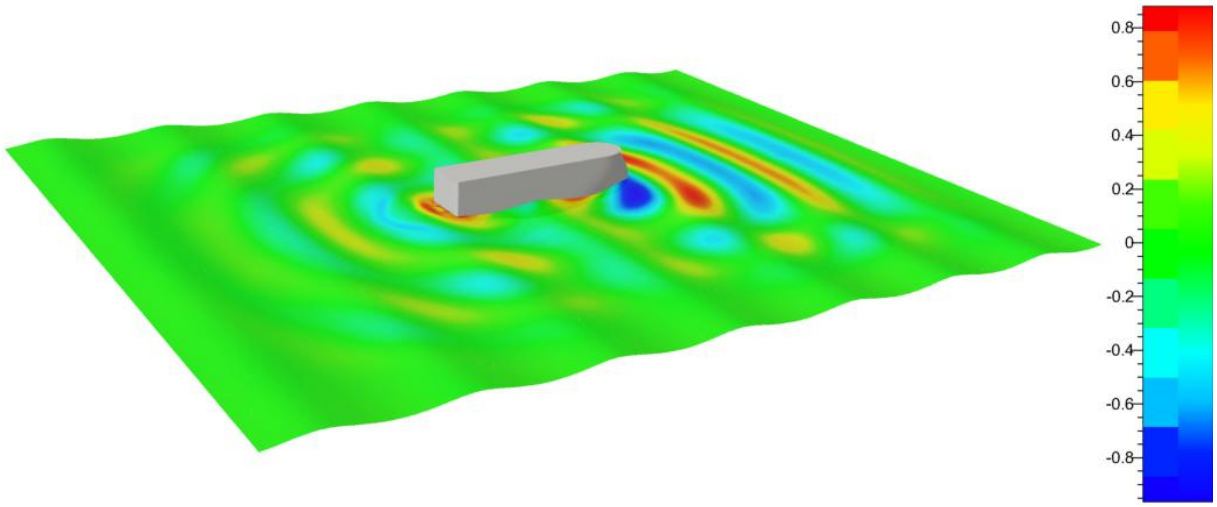

Fig. 9 Free surface colored by the diffracted wave elevation [m] for the case #02.

all around the solution, which is the actual numerical damping zone, canceling the diffracted waves only.

Calm water resistance was initially outside the scope of this CFD wave validation project. However, this topic is considered necessary in the validation process of added resistance in waves to ensure the viscous effects are taken into account properly. Without much efforts for the CFD user, results are meeting original expectations, proving that the method is well suited for steady cases as well. The free surface for the case #13 is shown on Fig. 10 where the results have been scaled back to full scale.

Getting correct predictions of the forces in waves (combined with vessel motions and flow visualizations) can be seen as the hydrodynamic Grail, opening the doors to optimization in waves, if computation time allows. Constantly looking for the right tool, Ulstein has made the choice to trust Lemma, and start the validation work even though ANANAS™ was still missing some key functionalities at the start (e.g. viscous layers' insertion, automatic scripts, etc.). The development team has shown to be very efficient at improving the tool, while Ulstein was familiarizing with the method and running the validation on non-viscous DP cases, which has been a success from the start. However, some skepticism was still present regarding the possibility to achieve such good results for transit in waves, where the physics is more complex. Once more, Ulstein has been positively surprised by the speed at which objectives have been reached. Indeed, only a couple of weeks have elapsed between the end of the software improvements and the end of this validation work. Both tasks were running simultaneously thanks to a good collaboration with the development team.

Results presented in Table 7 show pleasing agreement between experiments and CFD predictions. An example of 3D result is shown on Fig. 11 where the hydrodynamic pressure has been scaled back to full scale for the visualization.

Unfortunately, the expectations are not met for both cases #21 and #22. As discussed earlier, the case #21 was made to challenge both experiments and CFD by highlighting extreme slamming and green water. More importance was given to the visualization of green water for this case. Regarding the case #22, some disappointing differences remain between experiments and CFD predictions (13.6%). These differences are currently not explained but still under deeper investigations.

Now that satisfactory results have been achieved, one might notice that even if viscous simulations for transit in waves are fast, they still take about 3 times longer than non-viscous DP simulations that can give "overnight results". The main reasons being the heavier

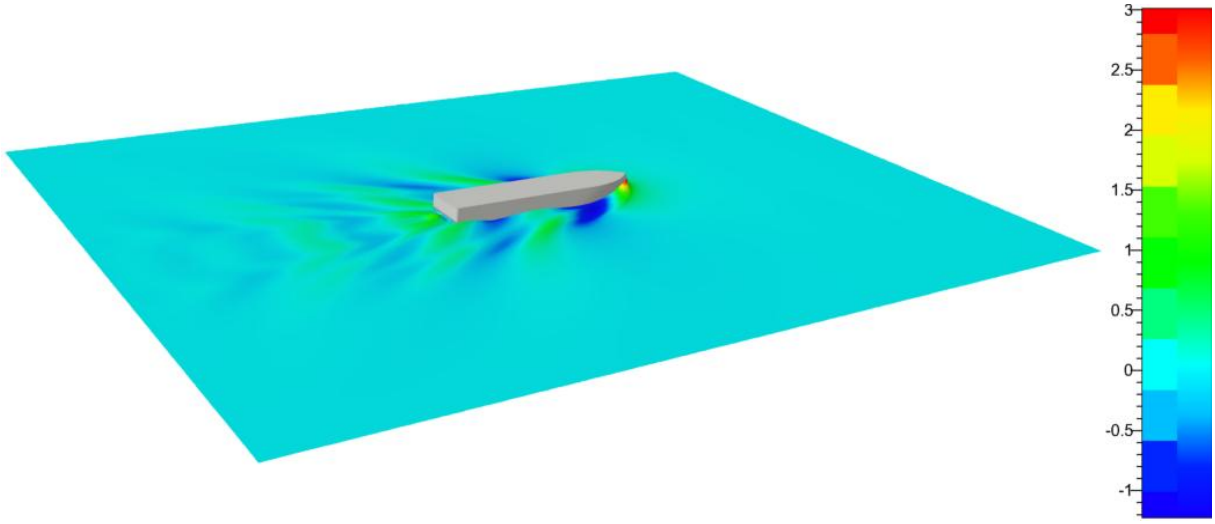

Fig. 10 Free surface colored by the total wave elevation [m] for the case #13.

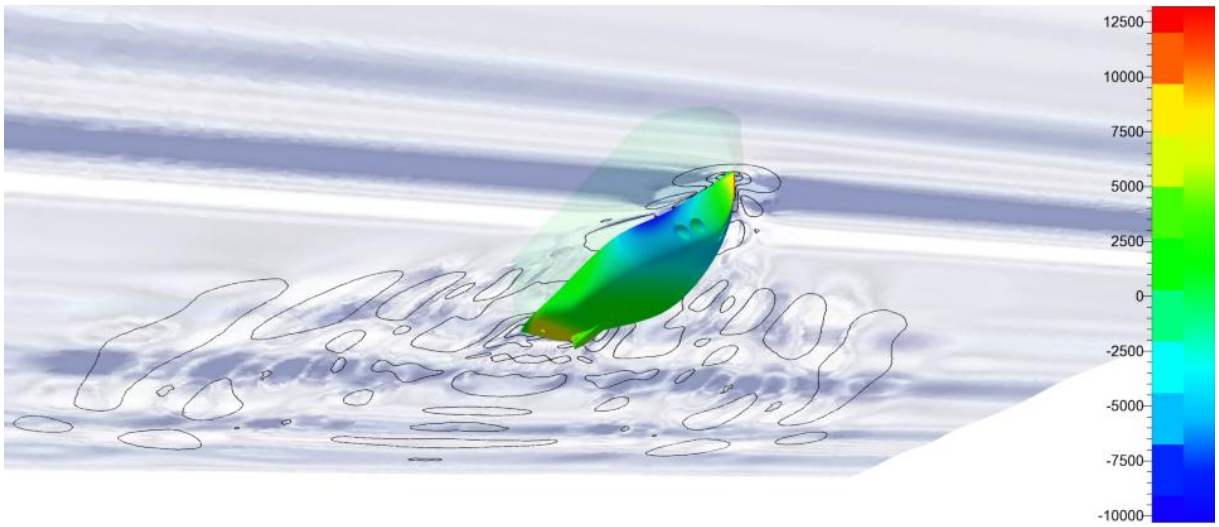

Fig. 11 Hull colored by the hydrodynamic pressure [Pa] and isocontours for the diffracted wave elevation for the case #19 in irregular waves.

mesh including viscous layers and the additional equations to solve in the system. As a consequence, such viscous calculations are now used in the final stage of the design process where accuracy is needed, while non-viscous calculations are used (with sufficient trust) to compare similar designs for both DP and transit in waves. The overall cluster capacity allows to compare 5 design variants per 24 hours in a given sea state.

6. Conclusions

Finding the right tool to perform such CFD simulations in waves has not been an easy task, and several tools have been considered and/or investigated along the entire research process that lasted for two and a half years. Ulstein sees in ANANAS™ a lot of potential, and it has achieved such a maturity that it is already being used for reliable predictions related to various commercial projects. On top of the achieved accuracy, computation time is a clear bonus of this method, so that systematic optimizations are being investigated at Ulstein.

One of the hard learnings of this project is that the results become very sensitive to the wave conditions when the wave length approaches the overall ship length. This is of course not something new, however, practical experience shows that an error of 2% on the wave period (that might seem insignificant) has led to 4% error on the wave length, changing the pitch response of the ship from 3 degrees to 2 degrees and causing a 10% underestimation on the average drag.

Looking at the long term use of ANANAS™ within Ulstein, other key topics are currently being investigated, such as amongst others, the flow inside moonpools with complex grids, the way the SWENSE method is dealing with green water, ships in oblique waves with smart roll damping models, and why not reducing the computation time even further in order to be able to deal with very complex geometries in a minimum amount of time. Even though these are still challenging topics today, the development team of Lemma is working hard on them with delivery expectations before the end of 2016.

7. Discussion

As an industry led research project, the focus has been on a robust solution for solving real problems, and not a purely academic program of work. This has created some challenges when it comes to the validation cases, where difficult conditions have been tested for specific cases in steep waves. These create a lot of spray and splashing making visual comparisons awkward. Some additional efforts were made to improve the visualization, without adverse effect to the

computation time. For Ulsteins' purposes the forces are the prime concern.

As stated, unfortunately, the expectations are not met for both cases #21 and #22. Regarding the case #22, (10 kt, head waves), the authors believe that these differences are due to some non-physical artefacts appearing in the solution causing a non-physical pressure peak normal to the vessel heading. This is under deeper investigation and shall be solved soon.

Extending this work into more market segments in the industrial context is the aim of the authors. Taking the simulations to higher speeds, Fn up to 0.4 is desirable and considered reasonable in the method. As opportunities present to be able to add more validation cases this should surely be done.

The validation was made with a standard hull for Ulstein. Which is not very slender, compared to a cruise ship, and in fact many vessels are quite fat, (low L/B ratios and small length displacement ratios) in the offshore segment. The method has no problem dealing with these. Where, for short fat vessels the relative motions become less reliable in heave and pitch for conventional methods in steep waves. In extreme sea states, the mesh deformation also increases. Some solve these complexities with overset mesh. ANANAS™ solves this in a different way, with re-meshing. The elegance of the mesh generator is that it is automated and should never fail and there are then no interfacing issues between users. It was not necessary to re-mesh in these validation cases, but it is anticipated that for larger waves and higher speeds this might be required.

Many offshore vessels are less standard, with considerable openings and recesses, like a moonpool or a well dock in the stern on a rescue vessel, landing platform dock or semi-submersible. This is a challenge for the SWENSE method for which a special development has been made to enable any opening to be modelled to allow for correct modelling of the wave reflections and incident wave. This is an opportunity enabling the SWENSE method to be exploited for more complex geometries.

Acknowledgments

We thank HSVA for providing Ulstein with reliable experiments and for being a high quality partner during this long term validation project.

References

[1] Luquet, R., Gentaz, L., Ferrant, P., and Alessandrini, B. 2004. "Viscous Flow Simulation Past a Ship in Waves Using the SWENSE Approach." 25th Symposium on Naval Hydrodynamics, St John's, Newfoundland and Labrador, Canada.

[2] Luquet, R. 2007. "Simulation numérique de l'écoulement visqueux autour d'un navire soumis à une houle quelconque." PhD thesis, Ecole Centrale de Nantes.

[3] Monroy, C. 2010. "Simulation numérique de interaction houle-structure en fluide visqueux par décomposition fonctionnelle." PhD thesis, Ecole Centrale de Nantes.

[4] Alessandrini, B., and Delhommeau, G. 1999. "A Fully Coupled Navier-Stokes Solver for Calculations of Turbulent Incompressible Free Surface Flow Past a Ship Hull." *International Journal for Numerical Methods in Fluid* 29: 125-42.

[5] Reliquet, G., Drouet, A., Guillerm, P. E., Jacquin, E., Gentaz, L., and Ferrant, P. 2012. "Simulation of Wave-Body Interaction by Coupling a Level-Set RANSE Solver and a Non-linear Potential Flow Solver." 13ième Journées de l'hydrodynamique.

[6] Dervieux, A., and Thomasset, F. 1981. "Multifluid Incompressible Flows by a Finite Element Method." *Lecture Notes in Physics* 11: 158-63.

[7] Osher, S., and Sethian, J. A. 1981. "Fronts Propagating with Curvature-Dependent Speed: Algorithms Based on Hamilton-Jacobi Formulations." *J. Comp. Phys.* 79 (1): 12-49.

[8] Lesage, A. C., Allain, O., and Dervieux, A. 2007. "On Level Set Modelling of Bi-Fluid Capillary Flow." *Int. J. Numer. Meth. Fluids* 53 (8): 1297-314.

[9] Koobus, B., Wornom, S., Camarri, S., Salvetti, M. V., and Dervieux, A. 2008. "Nonlinear V6 Schemes for Compressible Flows." Tech. Rep. RR-6433, INRIA.

[10] Francescatto, J., Dervieux, A., and Ravachol, M. 1997. "Efficiency of the Menter Correction for Steady and Unsteady Non Smooth Flows." *Second International Symposium on Turbulence Heat and Mass Transfer*, edited by Hanjalic, K., and Peeters, T. W. J. Delft University Press, 399-408.

[11] Hinze, J. 1959. *Turbulence.* New York: MacGraw-Hill.

[12] Guegan, D., Allain, O., Dervieux, A., and Alauzet, F. 2010. "An L∞–Lp Mesh-Adaptive Method for Computing Unsteady Bi-Fluid Flows." *Int. J. Num. Meth. Eng.* 84 (11): 1376-406.

[13] Sainte-Rose, B., Lenhardt, X., Allain, O., and Dervieux, A. 2012. "Numerical Study of the Turbulent Wake of a Towed or Auto-Propelled Axisymmetrical Body in a Stratified Medium Using LES-VMS." ASME FEDSM 2012-72413.

[14] Sirvinas, S., Allain, O., Wornom, S., Dervieux, A., and Koobus, B. 2006. "A Study of LES Models for the Simulation of a Turbulent Flow around a Truss Spar Geometry." 25th International Conference on Offshore and Arctic Engineering, Hamburg.

[15] Rienecker, M. M., Fenton, J. D., and Fourier, A. 1981. "Approximation Method for Steady Water Waves." *Journal of Fluid Mechanics* 104: 119-37.

[16] Det Norske Veritas (DNA). 2007. "Recommended Practice DNV-RP-C205, Environmental Conditions and Environmental Loads." April 2007.